Are Annulate Lamellae in the *Drosophila* Embryo the Result of Overproduction of Nuclear Pore Components?

JOEL P. STAFSTROM and L. ANDREW STAEHELIN
Department of Molecular, Cellular, and Developmental Biology, University of Colorado at Boulder, Boulder, Colorado 80309

ABSTRACT Annulate lamellae are cytoplasmic organelles composed of stacked sheets of membrane containing pores that are structurally indistinguishable from nuclear pores. The functions of annulate lamellae are not well understood. Although they may be found in virtually any eucaryotic cell, they occur most commonly in transformed and embryonic tissues. In *Drosophila*, annulate lamellae are found in the syncytial blastoderm embryo as it is cleaved to form the cellular blastoderm. The cytological events of the cellularization process are well documented, and may be used as temporal landmarks when studying changes in annulate lamellae. By using morphometric techniques to analyze electron micrographs of embryos, we are able to calculate the number of pores per nucleus in nuclear envelopes and annulate lamellae during progressive stages of cellularization. We find that annulate lamellae pores remain at a low level while nuclear envelopes are expanding and acquiring pores in early interphase. Once nuclear envelopes are saturated with pores, however, the number of annulate lamellae pores increases more than 10-fold in 9 min. Over the next 30 min it gradually declines to the initial low level. On the basis of these results, we propose (*a*) that pore synthesis and assembly continues after nuclear envelopes have been saturated with pores; (*b*) that these supernumerary pores accumulate transiently in cytoplasmic annulate lamellae; and (*c*) that because these pores are not needed by the embryo they are subsequently degraded.

Annulate lamellae are cytoplasmic organelles composed of stacked sheets of endoplasmic reticulum (ER)[1] membrane interrupted by annuli or pores. By all available criteria, except location, these pores are indistinguishable from nuclear pores, so both structures will be referred to interchangeably as "pores." In both systems, pores are known to have eightfold rotational symmetry within the plane of the membrane (8, 13). However, the high resolution structural methods recently applied to nuclear pores (35) have not yet been used to study annulate lamellae pores. Although pores are thought to be composed of both RNA and protein (5, 17, 27), no specific biochemical identity has yet been ascribed to a particular substructure. A 190-kilodalton glycoprotein from rat liver is the first protein to be uniquely associated with the pore complex (9), and this protein may be functionally analogous to a 174-kilodalton glycoprotein in the nuclear pore-lamina fraction of *Drosophila* embryos (3). Other evidence indicates that a protein found in the nuclear lamina also may be a component of the pore complex (32).

Annulate lamellae are found most commonly in embryonic or transformed cells (13, 15, 37), but they may also occur, albeit to a lesser degree, in virtually any eucaryotic cell at any time during its life history (22). Despite their ubiquity, our knowledge of annulate lamellae is limited. Although annulate lamellae are frequently cited in the literature (see references in 13, 15, 22, 37), few publications address in a precise way the dynamic formation and breakdown of these structures, or relate these changes to other events occurring concomitantly in the cell. Given the similarity of the two pore-containing membrane systems, it is not surprising that the nuclear envelope has been frequently implicated in the formation of annulate lamellae. Following mitosis, pieces of the fragmented nuclear envelope may be excluded from the re-forming nuclear envelope, giving rise to annulate lamellae in the cytoplasm or the nucleoplasm, the latter being the infrequently observed intranuclear annulate lamellae (1). In human oocytes, membranes may evaginate from the nuclear envelope directly, and become annulate lamellae as they acquire pores (10). Alternatively, the nuclear envelope may give rise to a large population of vesicles that are transported to some distal

[1] *Abbreviation used in this paper:* ER, endoplasmic reticulum.

THE JOURNAL OF CELL BIOLOGY · VOLUME 98 FEBRUARY 1984 699-708

site before they coalesce into annulate lamellae, a sequence of events supported by electron micrographs of oocytes of the amphibian *Necturus* and of other organisms (12, 13). The Golgi apparatus also has been implicated in the formation of annulate lamellae (21, 29). In dragonfly oocytes and *Drosophila* spermatids, dense cytoplasmic masses, possibly derived from the nucleus and containing ribonucleoprotein, have been postulated to be the immediate precursors of annulate lamellae pores (14, 16). This mechanism differs from the others referred to above by addressing the source of pore material, as opposed to membrane material, for the formation of annulate lamellae. Kessel (14–16) has noted further that protein synthesis occurs as annulate lamellae are formed, and he has proposed that the purpose for these pore structures may be to aid in the assembly of polysomes.

Annulate lamellae have been observed previously in the early *Drosophila* embryo both during normal development (19, 23), and following experimental manipulation (11). The great wealth of cytologic and genetic information available about this embryo makes it ideal for following dynamic changes in these or other organelles with great precision (6, 7, 18, 19, 24, 28, 38). We have documented very rapid and dramatic changes in the amount and structure of annulate lamellae during cellularization of the syncytial embryo. On the basis of our results, we propose that annulate lamellae in the *Drosophila* embryo transiently store excess pores before they are subsequently degraded.

MATERIALS AND METHODS

Handling Embryos: Eggs from rapidly laying wild-type *Drosophila melanogaster* females (strain Canton-S) were collected on laying plates at ~22°C (38). Under these conditions, eggs are fertilized in utero just before being laid, so a rather precise developmental age can be assigned to each embryo based on its morphology (24). Embryos ~2.0–3.5-h-old were used for these studies.

Fixation: Embryos were handled and fixed essentially as described by Zalokar and Erk (39), except for minor modifications. Embryos were dechorionated manually on double-stick tape, and floated on distilled water until they were of the proper age: embryos so treated developed normally through hatching. A solution containing 25% glutaraldehyde or 15% glutaraldehyde plus 10% acrolein in 0.1 M sodium cacodylate buffer (pH 7.2) was shaken with an equal volume of heptane, and embryos were fixed in the heptane phase for 1 min. They were then transferred to an aqueous fixative containing 2.5% glutaraldehyde, with or without 0.1% acrolein, for 1–2 h, during which time their vitelline membranes were removed with sharp tungsten needles. The same buffer at a concentration of 0.05 M was used for this and all subsequent steps. Washing in buffer (3 × 10 min) was followed by postfixation in buffered 1% OsO_4 for 1 h. Another series of washes was followed by en bloc staining in 1% aqueous uranyl acetate overnight at 4°C. Other than the en bloc staining, all steps were performed at room temperature. Dehydration was achieved through a series of ethanol and of propylene oxide; embedment was done in Epon-Araldite. A Reichert Ultracut microtome and DuPont diamond knife (DuPont Co., Wilmington, DE) were used to cut ribbons of silver sections. Sections were picked up on Formvar-coated slot grids, stained with uranyl acetate (1.5% in 70% methanol and 0.5% dimethyl sulfoxide) and Reynold's lead citrate, and stabilized with a thin layer of carbon. A JEOL 100C electron microscope was used for all observations.

Morphometric Calculations: Single cross sections of *Drosophila* embryos at various stages during cellularization were photographed in their entirety on several negatives, and printed at a total magnification of 4,000 diam. These micrographs were used to determine average values for the length, width, and center-to-center spacing of nuclei sectioned very nearly through their long axes; and the contour lengths of nuclear envelopes and annulate lamellae membranes.

The densities of pores in nuclear envelopes and in annulate lamellae (pores per square micrometer) were determined from tangential sections of these structures. Areas were calculated by cutting out enlargements of pore-containing membranes, weighing these pieces, and comparing their weights to those of known areas of identical photographic paper.

The surface area of nuclei was determined by assuming a simple model for their shape, namely, that of two hemispheres connected by a cylinder of equal diameter. If such a structure is sectioned through its long axis, then its perimeter, surface area, and volume can be calculated by merely knowing its width and length. The accuracy of this model can be tested by comparing the perimeter obtained by direct measurement (with a map wheel) with that predicted by the model for the same nuclei. At each stage, the actual perimeter was ~95% of that predicted by the model (93.2–96.7%). Knowing this error, we can approximate the actual surface area from that predicted by the model by multiplying the latter by the square of the error. We have used this method to estimate the surface area of the nuclei, which when taken together with the known pore density and the assumption of uniform pore distribution yields the approximate number of pores in a nucleus at each stage.

Annulate lamellae, defined here as cisternae of cytoplasmic membrane containing pores, occur in random orientations in the layer of cytoplasm that lies between the blastoderm nuclei at the embryo surface and the central yolk mass. Although individual lamellae or stacks of lamellae (as they are more commonly observed) are not associated with particular blastoderm nuclei, it is still possible to calculate the amount of annulate lamellae surface area and the number of annulate lamellae pores and express these values on a per nucleus basis. Then, since the numbers of pores in nuclear envelopes and in annulate lamellae are expressed in the same units, they may be compared readily.

Two methods have been used to estimate the number of annulate lamellae pores per nucleus. If similar values were obtained by each method, it would indicate that these values had a high probability of being correct, since each method of calculation relies on a different set of assumptions. By the first method, a theoretical cross-section of an embryo is considered in which nuclei are perfectly aligned and spaced. The average center-to-center spacing of nuclei is determined from measurements on thin sections of adjacent nuclei that are cut nearly through their long axes. If nuclei are assumed to be hexagonally packed (see Fig. 3*b*), the thickness of the theoretical thick section that contains only one row of nuclei and their accompanying cytoplasm will be sin 60°, or 0.866 times the lateral spacing. The number of nuclei that would fit in an embryo cross section of a given circumference is also calculated from the average lateral spacing. If annulate lamellae were aligned perpendicularly to the plane of the section, then their area within the volume of the theoretical section would be the product of their contour length in a representative thin section and the thickness of the theoretical section. However, since the angle of annulate lamellae planes relative to the plane of thin section appears to be random, a correction factor must be included in this equation. According to Underwood (34), a set of randomly oriented planes will occur at an average angle of 60° to the reference plane. The correction factor, then, has the value 1.155. This analysis gives an approximation of the total area of annulate lamellae membranes in a theoretical section. The number of annulate lamellae pores per nucleus is calculated by also knowing the density of pores in these membranes and the number of nuclei in the section. A rather large number of assumptions about the size, shape, and distribution of membranes and organelles were necessary to make the preceding calculations. However, this method does not suffer from the inherent sampling errors encountered in the following analysis.

The second method utilizes standard stereological principles. The surface area of a membrane-bounded structure per unit volume of cytoplasm, or S_v, is calculated by first counting the intersections between membrane profiles in a thin section and a pattern of test lines applied to this section, and then using appropriate formulas. An important aspect of this analysis is that it "applies to systems of surfaces with any configuration" (34). Rather than calculating actual values of S_v for annulate lamellae and nuclear envelopes, we instead determined the ratio of these values directly. This ratio is the quotient of membrane contour lengths measured with a map wheel. From this ratio and the known surface area of nuclei (see above), we can calculate the area of annulate lamellae membranes per nucleus. The number of annulate lamellae pores per nucleus, then, is a product of this area and the density of pores in annulate lamellae. This method requires relatively few measurements or calculations compared with the first method, but an inherent caveat of it is that objects are assumed to be oriented with complete randomness, a condition that is not fully met by nuclei that are always sectioned parallel to their long axes.

Freeze-Fracture: Embryos were collected, dechorionated, and aged as for chemical fixation. They were then sandwiched between two copper "hats," using slot grids of appropriate thickness as spacers, and ultrarapidly frozen in a propane jet freezer. Frozen embryos were fractured, etched slightly, and replicated with platinum/carbon in a Balzers freeze-etch machine (Balzers, Hudson, NH). Replicas were cleaned with commercial bleach and 70% H_2SO_4, picked up on mesh grids, and observed as for sections.

RESULTS

The typical structure of annulate lamellae in cross and tangential sections is depicted in Fig. 1. Parallel layers of double

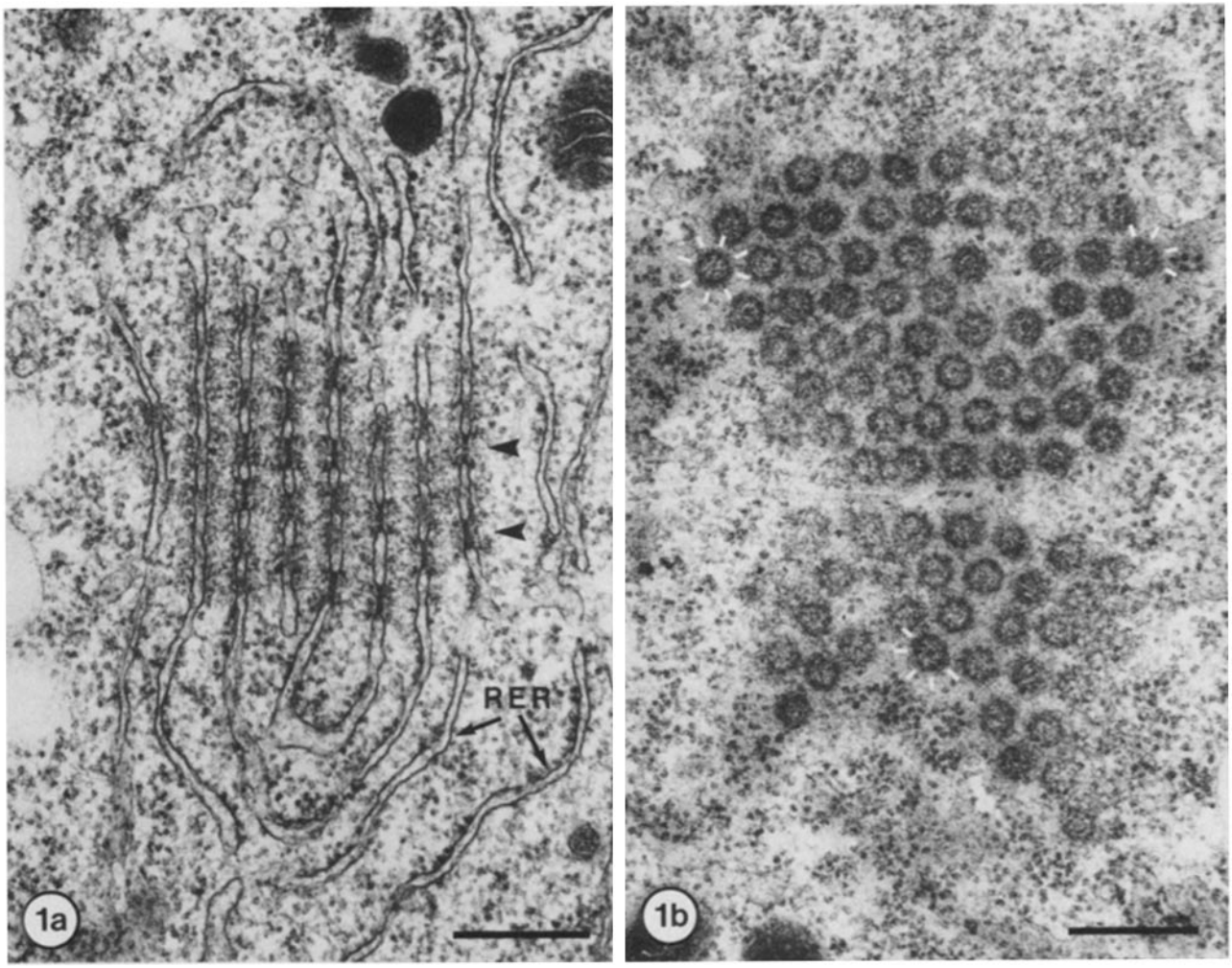

FIGURE 1 Annulate lamellae structures. (*a*) A cross section reveals that lamellae are aligned in a precise, parallel array, that pores (arrowheads) in adjacent lamellae also are aligned, and that lamellae are interconnected by rough ER (*RER*). (*b*) Pores occur at high density and are hexagonally packed in this tangential section. The large central granule and smaller annular granules (white dashes) seen in some pores are also characteristic features of nuclear pores. Bars, 0.5 μm. (*a*) × 38,000; (*b*) × 36,000.

membrane are interrupted by a large number of pores and are interconnected by ER membranes lacking pores, but having attached ribosomes (Fig. 1*a*). These connecting membranes are similar to the ones seen to interconnect discrete annulate lamellae structures (see Fig. 6*b*). Pores within adjacent lamellae are frequently aligned, as is also seen when annulate lamellae appear to be just forming (see Fig. 5*c*). It seems likely that this apparent affinity between pores is what causes the layers of annulate lamellae to be assembled into structures with such precise geometry. In tangential section, the high density and nearly perfect hexagonal packing of pores is evident (Fig. 1*b*). In pores sectioned appropriately, a large central granule and smaller annular granules are observed. Nuclear pores viewed in the same orientations exhibit the same structural features as annulate lamellae pores (data not shown).

The similarity of pores in annulate lamellae and nuclear envelopes is emphasized further by their appearance in freeze-fracture (Fig. 2). The density of nuclear pores is quite high, but pores do not assume any particular packing configuration (Fig. 2, *a* and *b*). Pores of annulate lamellae, on the other hand, have the tendency to aggregate into hexagonal arrays (Fig. 2*c*), as was also seen in thin section (Fig. 1*b*). The annulate lamellae structure depicted in Fig. 2*c* is from an embryo in late interphase preceding the last syncytial nuclear division; its small size is characteristic of this stage (unpublished observations). Although freeze-fracture micrographs do not immediately reveal a great deal of information about pore substructure, both types of pores do exhibit eightfold rotational symmetry when printed by the Markham technique (20) to enhance this symmetry (data not shown).

Light micrographs of an embryo in an early stage of cellularization provide a global view of the *Drosophila* embryo (Fig. 3). Blastoderm nuclei are seen to be densely packed at the embryo surface, with a thick layer of cytoplasm lying between these nuclei and the central yolk mass (Fig. 3*a*). Cleavage furrows originating at the embryo surface generally advance inward to a uniform depth around the entire embryo. In this embryo, furrows have reached a point about one-third of the way along the radially elongated nuclei, indicating that this embryo is slightly younger than the embryo depicted in Fig. 5. Embryo cross sections of roughly equivalent area were used for the electron microscopic analysis described below. A grazing section of the same embryo (Fig. 3*b*) demonstrates that nuclei are nearly hexagonally packed, that is, most nuclei have six others as nearest neighbors while a few other nuclei have either five or seven. Although no pole cells are evident, both sections are from the posterior end of the embryo.

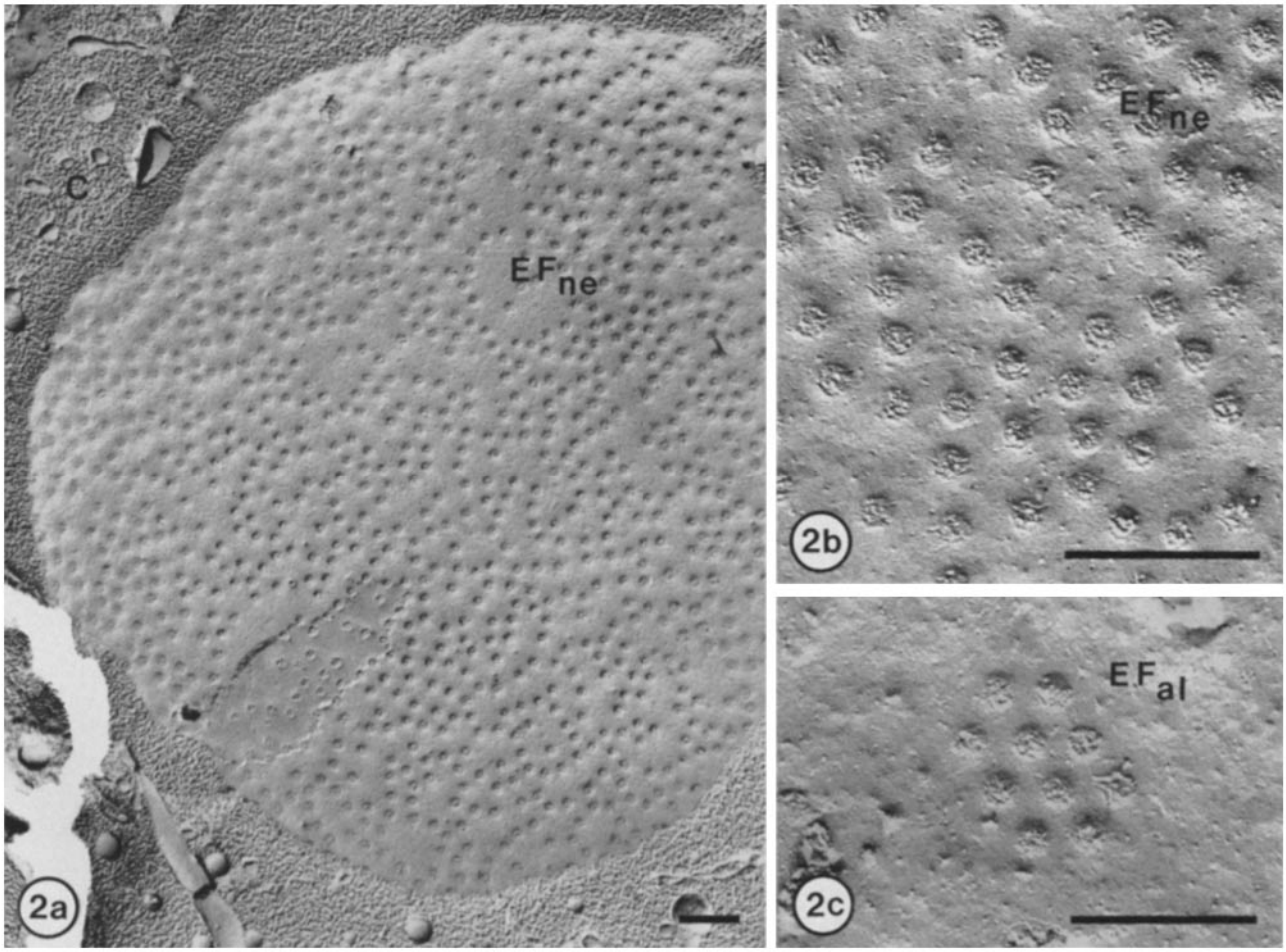

FIGURE 2 Freeze-fracture micrographs of an embryo in late interphase preceding the last syncytial nuclear division. (*a* and *b*) The nuclear envelope contains pores at a rather high density, but they do not assume any particular packing configuration. (*c*) Pores in annulate lamellae are very similar to those in the nuclear envelope, but usually are hexagonally packed. The small size of this structure is characteristic of this early stage. (C, cytoplasm; EF_{al}, EF fracture face of an annulate lamellae cisterna; EF_{ne}, EF fracture face of the outer nuclear envelope). Bars, 0.5 μm. (*a*) × 16,000; (*b* and *c*) × 50,000.

The events of cellularization, like those of nuclear division, occur with a high degree of synchrony throughout the *Drosophila* embryo (see Fig. 3). Although we do not know the exact developmental age of a particular embryo, an approximate age has been assigned to each based on its morphology using the data of Rabinowitz (24). 144 min after a fertilized embryo has been laid, 13 nuclear divisions have been completed, and some 6,000 small, early interphase nuclei are found virtually close-packed just beneath the embryo surface (Fig. 4). Cleavage furrows originating at the surface envelop these blastoderm nuclei, which elongate toward the embryo center as they increase in volume. At 171 min, furrows have proceeded halfway along the elongated nuclei (Fig. 5 *a*), and by 180 min they have reached the bases of these nuclei (Fig. 6 *a*). Furrows continue to grow inward, now at an increased rate, until they approach the central yolk mass, thus forming the cellular blastoderm at 186 min (Fig. 7 *a*). Cell migrations, such as those that give rise to the ventral furrow, follow and mark the onset of gastrulation at ~210 min (Fig. 8 *a*). A more complete description of cellularization is available elsewhere (6, 7, 19).

The stages of cellularization described above are easily recognized, and may be used as convenient reference points when studying other dynamic events occurring in these embryos. One such dynamic event is the formation and subsequent disappearance of annulate lamellae. The relative abundance and location of these organelles can be discerned in low power micrographs, while details of their structure are evident only at higher magnification. Very few annulate lamellae are present during the earliest stages of furrow growth between 144 min and 171 min (Figs. 4 and 5 *a*). The structures observed at 171 min are composed of only one or two membrane layers, and contain only a few pores (Figs. 5, *b* and *c*). Pores in adjacent lamellae may already be aligned, and Golgi cisternae are frequently observed near these forming structures (Fig. 5 *c*). At 180 min, only 9 min later, the number and form of annulate lamellae have changed considerably. A large number of obvious structures are present, predominantly in the region of the cytoplasm near the edge of the yolk mass (Fig. 6 *a*). These structures are composed of several layers of stacked lamellae, each containing a large number of pores. In addition, stacks are interconnected by cisternae of rough ER lacking pores (Fig. 6 *b*). A considerable number of annulate lamellae remain when cellularization is complete at 186 min, but it is evident that they have begun to decline by this stage (Fig. 7 *a*). It is also evident from Fig. 7 *a* that annulate lamellae are largely excluded from the newly formed cells, even though cytoplasmic connections persist between the cells and the yolk. Annulate lamellae still occur as well developed stacks at 186 min, but, in addition, ER-like

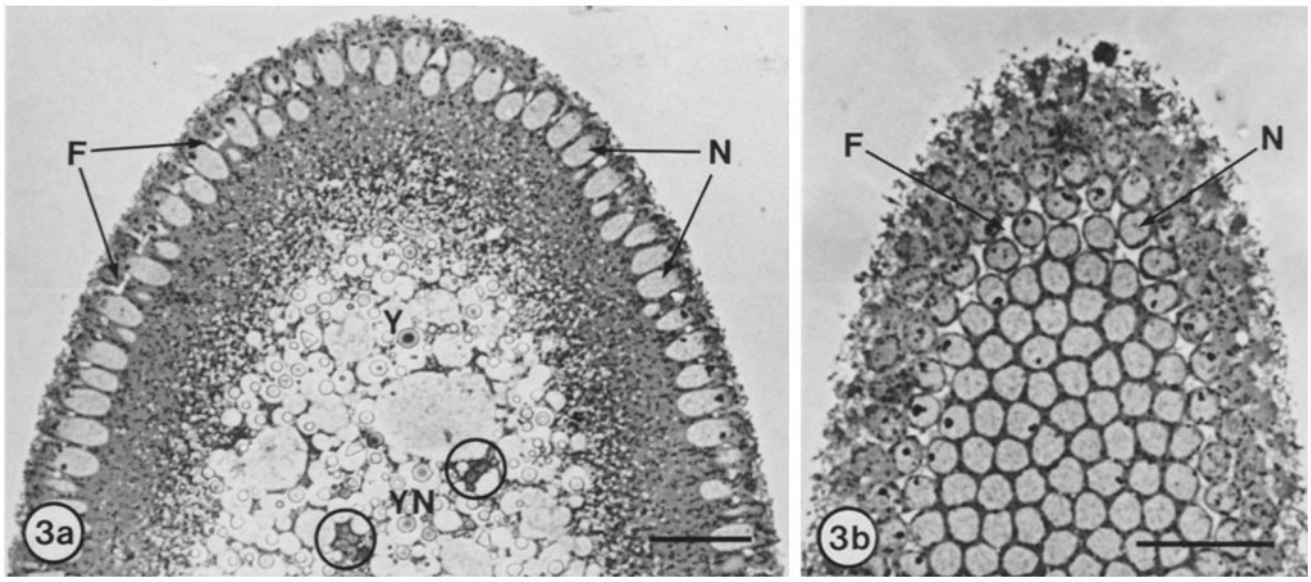

FIGURE 3 Phase contrast light micrographs of plastic embedded thick sections stained with toluidine blue. Both micrographs are of longitudinal sections of the posterior end of a 168-min embryo. (*a*) Cleavage furrows (*F*), which have originated at the embryo surface, have advanced about one-third of the way along elongated blastoderm nuclei (*N*). A thick layer of cytoplasm lies between these nuclei and the central yolk mass (*Y*), which also contains a few yolk nuclei (*YN*). (*b*) A grazing section of the embryo demonstrates the close, near hexagonal packing of blastoderm nuclei. The white areas between the more peripheral nuclei represent the dilated tips of the cleavage furrows. Nuclei nearer to the center of the micrograph have been sectioned at a deeper level in the embryo where cleavage furrows have not yet reached. Bars, 25 μm. (*a*) × 540; (*b*) × 750.

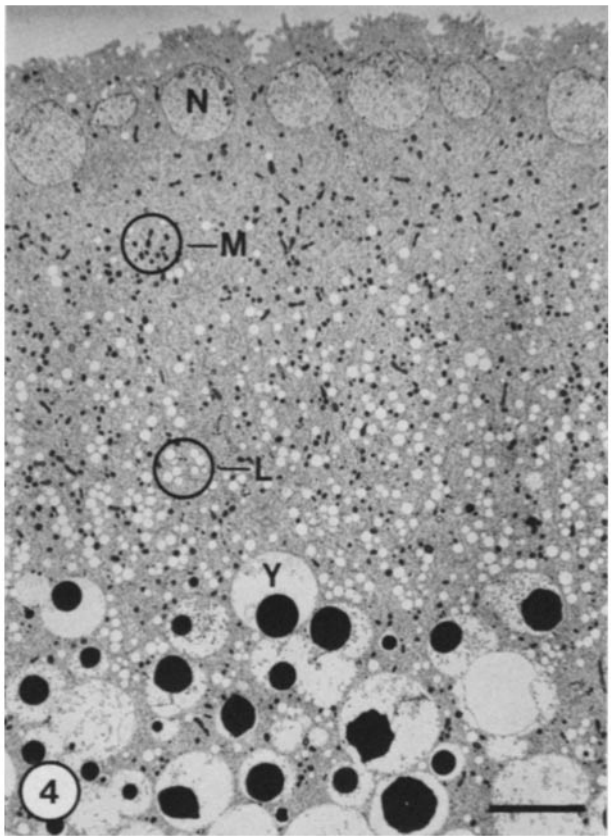

FIGURE 4 Cross section of a 144-min embryo. Small, round, early interphase nuclei lie just beneath hillocks of microvilli on the embryo surface. Annulate lamellae occasionally may be found at this stage, although none are present in this micrograph. (*L*, lipid; *M*, mitochondria; *N*, blastoderm nucleus; *Y*, yolk granule). Bar, 5 μm. × 2,500.

membranes with circular profiles are often associated with one or both faces of a stack. These membrane circles generally contain pores only where they face an annulate lamellae stack (Fig. 7*b*). By early gastrulation (210 min), annulate lamellae are again scarce and are composed of only a couple of lamellae (Fig. 8). Membrane circles are more common than they were in the previous stage, and again are found predominantly in the region of the degenerate annulate lamellae (Fig. 8*b*). It is possible that these membrane circles represent membrane material previously contained in annulate lamellae stacks. The exact fate of pores following annulate lamellae breakdown is unknown.

Data collected from considerably larger areas of the same embryos depicted in Figs. 4–8 are presented in Table I. The measured frequencies substantiate that the largest number of annulate lamellae and the greatest total contour length of these membranes occur in the 180-min embryo. Also, the greatest proportion of these structures at all stages is found in the cytoplasm at the edge of the central yolk mass, not in association with either yolk nuclei, as suggested by Mahowald (19), or blastoderm nuclei.

The number of pores in nuclear envelopes and annulate lamellae, each on a per nucleus basis, was calculated as described in Materials and Methods using the data presented in Table II. Notice that the values for annulate lamellae pores per nucleus calculated by two different methods are very similar. The most relevant of these data are presented graphically in Fig. 9. The number of nuclear envelope pores rises as the surface area of the nucleus increases between 144 min and 171 min, and then both remain nearly constant through early gastrulation at 210 min. The number of pores associated with annulate lamellae remains low while the enlarging nuclear envelope is still acquiring pores (144 min to 171 min), but increases more than 10-fold in the short interval immediately thereafter (171 min to 180 min). The number of

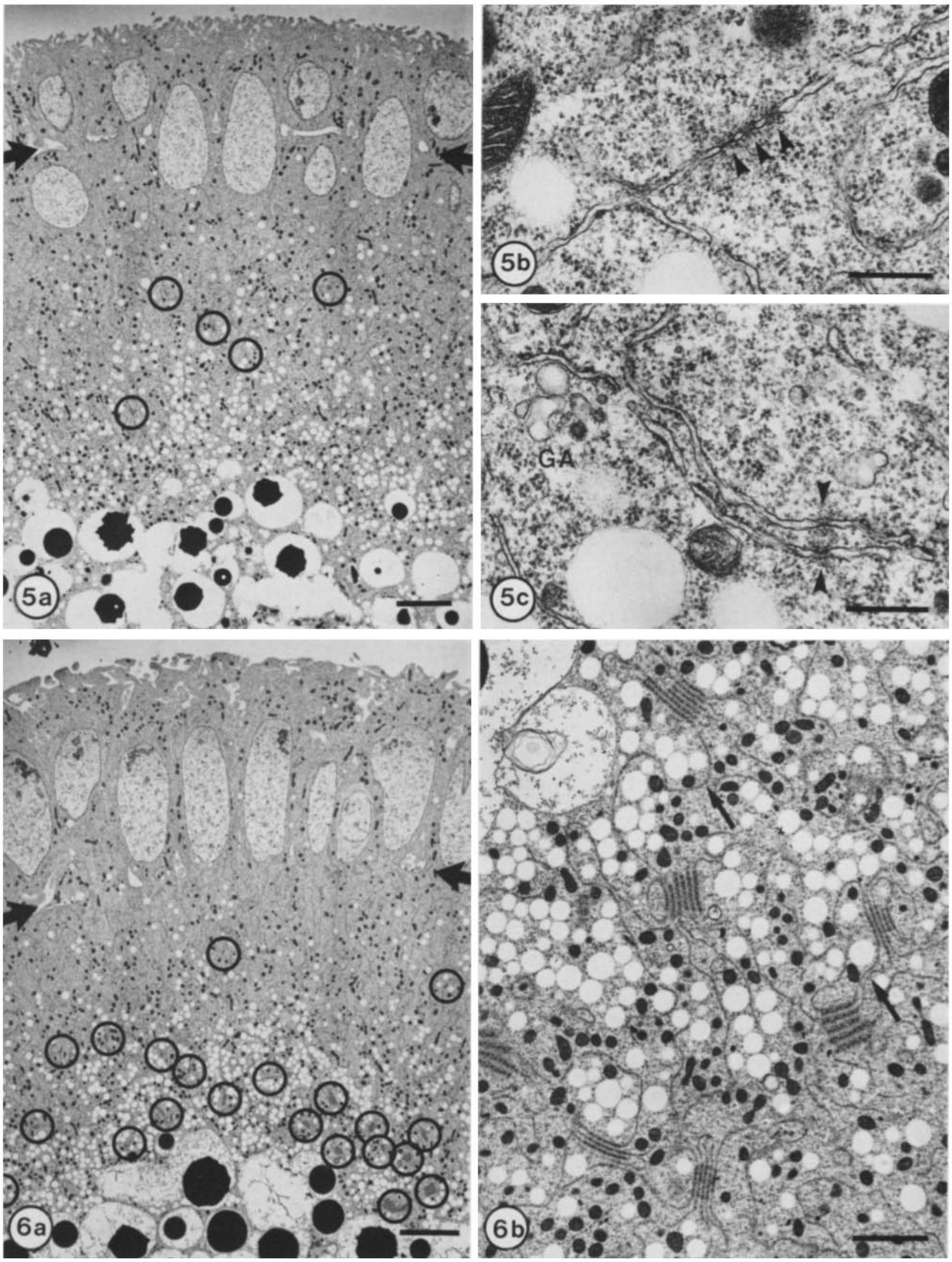

along the elongated nuclei. A few small annulate lamellae are present (circles). (*b* and *c*) Annulate lamellae are composed of only one or two cisternae and contain only a few pores (arrowheads). Golgi apparatus (*GA*) commonly are seen near these apparently forming structures. Bars, (*a*) 5 μm; (*b* and *c*) 0.5 μm. (*a*) × 2,150; (*b* and *c*) × 29,000. Fig. 6: Cross sections of a 180-min embryo. (*a*) Cleavage furrows (arrows) have reached the bases of the elongated nuclei. A large number of annulate lamellae are in the cytoplasm near the central yolk mass (circles). (*b*) Annulate lamellae are composed of several cisternae and contain pores at a high density. Stacks of annulate lamellae are interconnected by membranes lacking pores (arrows). Bars, (*a*) 5 μm; (*b*) 2 μm. (*a*) × 2,150; (*b*) × 6,700.

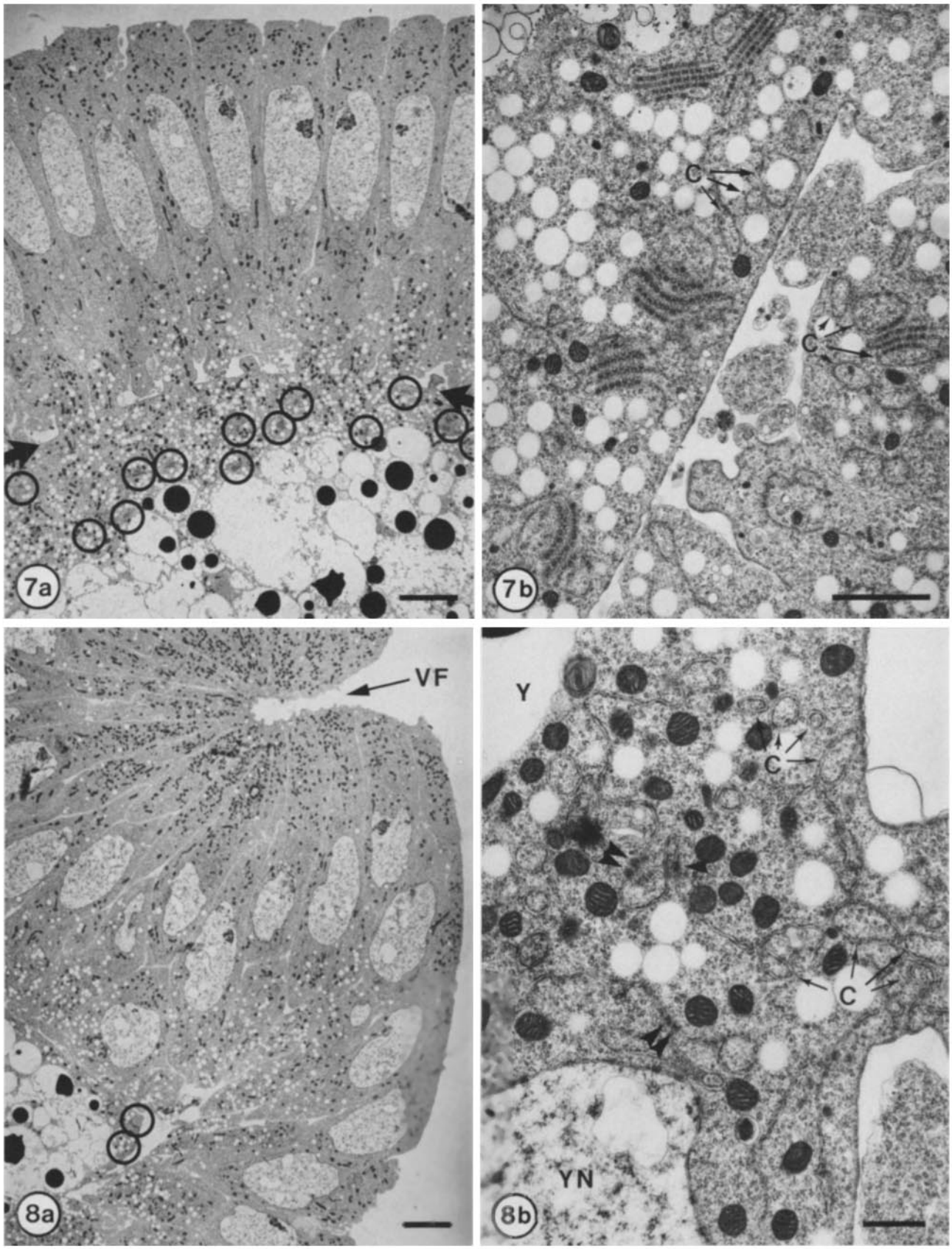

to form the cellular blastoderm. Several annulate lamellae are near the yolk mass (circles) but few are found within the nascent cells, even though cytoplasmic connections persist. (*b*) ER-like membranes with circular profiles (*C*) are common near annulate lamellae structures, and they may contain pores where they are adjacent to an annulate lamellae stack. Most annulate lamellae are excluded from the nascent cells, at right. Bars, (*a*) 5 μm; (*b*) 2 μm. (*a*) × 2,150; (*b*) × 8,800. Fig. 8: Cross sections of a 210-min embryo. (*a*) An inward migration of cells along the ventral surface of the embryo leads to the formation of the ventral furrow (*VF*), an early event in gastrulation. Only a few annulate lamellae are present, most commonly among the yolk (circles). (*b*) Pores are observed only rarely in cytoplasmic membranes (arrowheads), while membranes with circular profiles (*C*) have become more common. (*Y*, yolk granule; *YN*, yolk nucleus). Bars, (*a*) 5 μm; (*b*) 1 μm. (*a*) × 1,750; (*b*) × 11,000.

annulate lamellae pores then declines more gradually, and returns to the initial low level by early gastrulation (210 min).

DISCUSSION

The primary data presented here on pore dynamics are based on measurements from single cross sections through single embryos at each stage. However, each section assayed represents an area of at least 10,000 square micrometers, a rather large sample. We believe that the general conclusions that we draw from these data are valid, and that the specific values for pore quantities that we have calculated represent good approximations for the actual values. The latter point is strengthened by the fact that we arrived at very similar values for the number of annulate lamellae pores per nucleus by two different methods of calculation (Table II). Also, all observations have been confirmed qualitatively on other sections of the same embryos, and on other embryos at similar stages. The value of this type of information may be appreciated by merely counting the annulate lamellae structures in the low magnification micrograph of each stage (Figs. 4–8; Table I). Similarly, Rickoll (25) presents micrographs of stages of ventral furrow formation between our 186- and 210-min stages that support a trend of annulate lamellae breakdown during this time, as we have documented. In the earlier stage, a few small annulate lamellae structures are seen, while none are evident in the later stage (Rickoll's Figs. 5 and 6, respectively).

In the syncytial *Drosophila* embryo, 13 nearly synchronous nuclear divisions give rise to some 6,000 surface or blastoderm nuclei in ~2½ h (33, 38). Division cycles are very short, lasting on the average 10 min for the first nine and 15 min for the last four. Observations on living embryos confirm that the cell cycle rate is somewhat faster in early divisions and slower in later ones (4, 36), perhaps because structural or informational molecules needed in the division process are being exhausted, or cannot be synthesized fast enough to keep pace with an exponentially increasing demand for them. Nuclear pores occur at high densities even during late syncytial divisions (Fig. 2*a*; Table II), so pore material must either be synthesized, or recruited from some storage organelle during this period of rapid nuclear growth. Our data suggest that nuclear pores are being synthesized at this time since annulate lamellae, a strong candidate for the hypothetical storage organelle, do not occur in sufficient numbers before cellularization to account for the number of pores needed by 6,000 nuclei. When annulate lamellae are most abundant (180 min), the number of pores they contain on a per nucleus basis is nearly equivalent to the number of pores in an early interphase nucleus (Fig. 9; Table II). Thus, if all of these nuclear pores were stored in annulate lamellae they should be abundant and clearly visible in early stages of embryogenesis. Pore material could be stored in other forms such as the dense cytoplasmic masses described by Kessel (14, 16), but such material was never observed in our specimens, even when annulate lamellae apparently were being formed (Fig. 5). Since the number of nuclei doubles at each division, the number of pores needed to fill their nuclear envelopes should increase

TABLE I

Contour Length and Distribution of Annulate Lamellae

	144 min	171 min	180 min	186 min	210 min
No. of nuclei*	72.4	53.5	41.7	46.4	46.6
Contour length of AL (μm)					
Yolk	0	0	7.1	3.3	0
Cytoplasm‡	11.9	21.6	198.6	116.8	9.9
Cells	—	—	—	8.9	0.5
TOTAL	11.9	21.6	205.7	129.0	10.4
Distribution of AL stacks					
Yolk	0	0	7	3	0
Cytoplasm‡	23	28	70	36	11
Cells	—	—	—	8	2
TOTAL	23	28	77	47	13
Average length of AL per stack (μm)	0.52	0.77	2.67	2.74	0.80

* See Materials and Methods.
‡ Cytoplasm between the edge of the central yolk mass and blastoderm nuclei in early stages or the bases of cells in late stages.
AL, annulate lamellae.

TABLE II

*Nuclear Envelope and Annulate Lamellae Pores**

	144 min	171 min	180 min	186 min	210 min
NE pores					
NE surface area (μm²)	66.0	153.1	157.0	167.4	166.4
NE pore density (per μm², ± SD)	16.61 ± 0.69	12.01 ± 1.11	9.90 ± 0.85	9.65 ± 1.60	11.85 ± 1.86
NE pores per nucleus	1,096	1,839	1,554	1,615	1,972
AL pores					
AL contour length (μm)	11.9	21.6	205.7	129.0	10.4
thickness of theoretical section (μm)	4.62	5.30	5.54	5.07	5.20
total AL area (μm²)‡	63.5	132.2	1,316.2	755.4	62.5
AL pore density (per μm², ± SD)§	26.41 ± 1.25	26.41 ± 1.25	26.41 ± 1.25	26.41 ± 1.25	26.41 ± 1.25
number of nuclei	72.4	53.5	41.7	46.4	46.6
AL pores per nucleus—theoretical section (first method)	23.2	65.3	833.6	430.0	35.4
AL pores per nucleus—stereology (second method)‖	27.5	66.6	805.5	387.2	34.6

* See Materials and Methods.
‡ Includes angular correction factor of 1.155.
§ Determined from 180-min and 186-min embryos.
‖ Data for these calculations not shown.
AL, annulate lamellae; *NE*, nuclear envelope.

accordingly. It is obvious, then, that pore synthesis would have to be controlled rigorously to meet the demand for pores precisely. Nuclear division might be slowed if pore synthesis were too slow, or pores might accumulate if they either were synthesized too rapidly or continued to be synthesized after the demand for them was met.

The pores found in nuclear envelopes and in annulate lamellae membranes appear to be identical by all available morphological and biochemical criteria (Figs. 1, 2; references 5, 13–15, 22, 37), and the data presented here suggest that these two populations of pores are related kinetically as well (Fig. 9). Indeed, the function of annulate lamellae in the *Drosophila* embryo may be that of a transient storage organelle for excess nuclear pores. Nuclear envelopes gain pores in early interphase as their surface area is expanding. Once nuclear envelopes are "saturated" with pores, however, pores that are still being synthesized may be assembled and accumulate in an analogous way in other membranes with a similar affinity for them, thereby forming cytoplasmic annulate lamellae. At this time, we have no information about any cellular factor or factors that might, first, recognize that nuclear envelopes contained a sufficient number or density of pores and disallow further accumulation, and, second, make cytoplasmic membranes receptive to acquiring them. If the pores in annulate lamellae actually represent a waste product of over-synthesis, then their subsequent degradation would be the logical next step. Since annulate lamellae are largely excluded from the newly formed cells (Figs. 7 and 8; Table I), it is unlikely that they serve any important function in these cells. It thus appears that the synthesis of pores in the *Drosophila* embryo may not be finely controlled. However, the energetic cost of this overproduction, which amounts to nearly enough pores to accommodate another generation of early interphase nuclei, may be small when measured against the consequences of having an inadequate number of pores in the nuclei of these embryonic cells. Also, while the embryo's demand for pores increases exponentially during nuclear division, it ends abruptly with the onset of cellularization. It therefore is not surprising that pore synthesis would continue for some time after the demand for pores had been met. Our interpretation of these events is summarized in Fig. 10.

We have previously shown that nuclear envelopes remain largely intact during nuclear division in the syncytial *Dro-*

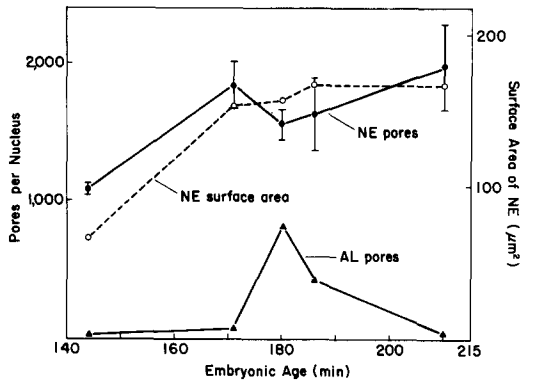

FIGURE 9 Number of pores in nuclear envelopes (± SD) and in annulate lamellae (calculated by the first method), each on a per nucleus basis, and nuclear surface area during cellularization of the *Drosophila* embryo. Nuclear pores increase as the nuclear envelope expands between 144 and 171 min, and then both remain nearly constant. Annulate lamellae pores remain at a low level while nuclear envelopes are acquiring pores, and then, between 171 and 180 min, their number increases dramatically. Annulate lamellae pores subsequently decline more gradually.

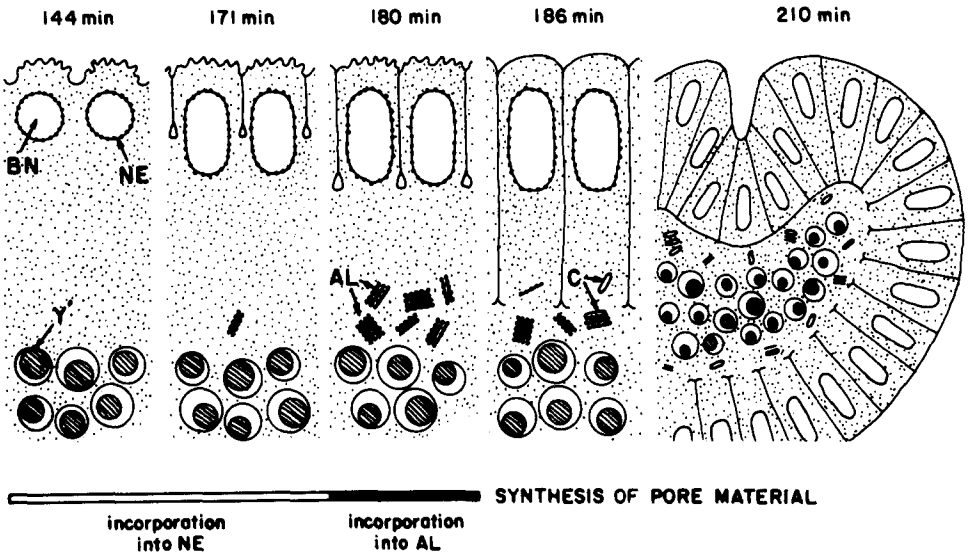

FIGURE 10. Diagram summarizing our interpretation of nuclear pore dynamics during cellularization of the *Drosophila* embryo. Pore material is synthesized between 144 and 180 min. During the first phase of this interval (144–171 min), nuclear envelopes (*NE*) of blastoderm nuclei (*BN*) are expanding and acquiring pores. After this time, nuclear envelopes are saturated with pores, so pores synthesized between 171 and 180 min accumulate in cytoplasmic membranes instead, and form annulate lamellae (*AL*) near the edge of the central yolk mass (*Y*). These annulate lamellae are largely excluded from the newly formed cells of the cellular blastoderm (186 min) and, thus, probably serve no useful function in these cells. The number and total length of annulate lamellae have begun to decline by this time. The membrane component of annulate lamellae appears to be transformed into membranes with circular profiles (*C*), and while the exact fate of the pores is unknown, it is presumed that they are degraded. At 210 min, as the ventral furrow is being formed, very few annulate lamellae remain, and of these, few are found in blastoderm cells. Membrane circles, however, are more common than at the previous stage.

sophila embryo, and, in addition, that these envelopes lose their pores and become fenestrated (30). We were intrigued by the possibility that these pores might transiently accumulate in annulate lamellae. To the contrary, however, pores in the few small annulate lamellae found at this time are disassembled in an analogous manner and with the same timing as those of blastoderm nuclear envelopes (31).

The hypothesis that the function of annulate lamellae is to store nuclear pores, and perhaps nuclear membrane material as well, is not without precedent. In the foraminifer *Hastigerina pelagica,* a single, large gamont nucleus divides in 2–4 h into ~300,000 gamete nuclei, with 60–70 times more surface area (29). Before these divisions occur, a large amount of annulate lamellae accumulates around the gamont nucleus and apparently becomes incorporated into the nuclear envelopes of the gametes. It seems likely that the rate of division could not be so rapid if nuclear envelope material were not synthesized in advance and stored as annulate lamellae. It appears, then, that nuclear pores accumulate transiently in annulate lamellae in both *H. pelagica* and the *Drosophila* embryo. In the former the stored pores are needed and will soon be used, while in the latter they are superfluous and will be degraded. Since annulate lamellae occur most commonly in embryonic and transformed tissues (13, 15, 22, 37), sites where cells exhibit high rates of division and metabolism, annulate lamellae may always accumulate pores either in advance of a need for them or after such a need has been filled, but synthesis continues.

Kessel (14–16) has proposed quite a different hypothesis for the function of annulate lamellae observed during oogenesis in dragonflies and spermatogenesis in *Drosophila.* The fundamental assumptions of this hypothesis are that a normal function of the nuclear pore is to aid in the assembly of functional polysomes and thereby promote protein synthesis, and that annulate lamellae pores amplify this function when high rates of protein synthesis are required. Although annulate lamellae do appear in these systems when protein is being synthesized actively, there is no evidence for direct causality between these events. More importantly, from what we know now about the initiation of translation of both soluble and membrane-associated proteins (2, 26), it is quite unlikely that pores are involved in this process. This view is further substantiated by the fact that cell-free translation systems require neither pores nor any other nuclear envelope–associated factor to synthesize protein accurately and at good rates.

In summary, all of the data presented here support the hypothesis that the function of annulate lamellae in the *Drosophila* embryo is to transiently store or accumulate excess nuclear pore material. Since these pores serve no apparent purpose in the cellular embryo, they are subsequently degraded.

We would like to gratefully acknowledge Dr. Larry Goldstein for aiding us with all aspects of *Drosophila* biology, and for commenting on the manuscript; Dr. Richard McIntosh for helpful criticism on our stereological methods and on the manuscript, and for allowing us to use his light microscopes; and Ms. Jan Logan for preparing the diagrams.

This work was supported by National Institutes of Health grant GM 18639 to L. A. Staehelin.

Received for publication 16 June 1983, and in revised form 24 October 1983.

REFERENCES

1. Afzelius, B. A. 1955. The ultrastructure of the nuclear membrane of the sea urchin oocyte as studied with the electron microscope. *Exp. Cell Res.* 8:147–158.
2. Blobel, G. 1980. Intracellular protein topogenesis. *Proc. Natl. Acad. Sci. USA* 77:1496–1500.
3. Fisher, P. A., M. Berrios, and G. Blobel. 1982. Isolation and characterization of a proteinaceous subnuclear fraction composed of nuclear matrix, peripheral lamina, and nuclear pore complexes from embryos of *Drosophila melanogaster. J. Cell Biol.* 92:674–686.
4. Foe, V. E., and B. M. Alberts. 1983. Studies of nuclear and cytoplasmic behavior during the five mitotic cycles that preceed gastrulation in *Drosophila* embryogenesis. *J. Cell Sci.* 61:31–70.
5. Franke, W. W., and U. Scheer. 1974. Structures and functions of the nuclear envelope. *In* The Cell Nucleus, Vol 1. H. Busch, editor. Academic Press, New York. pp. 220–347.
6. Fullilove, S. L., and A. G. Jacobson. 1971. Nuclear elongation and cytokinesis in *Drosophila montana. Dev. Biol.* 26:560–577.
7. Fullilove, S. L., and A. G. Jacobson. 1978. Embryonic development: descriptive. *In* Genetics and Biology of Drosophila Vol 2c. M. Ashburner and T. R. F. Wright, editors. Academic Press, London. pp. 105–227.
8. Gall, J. 1967. Octagonal nuclear pores. *J. Cell Biol.* 32:391–399.
9. Gerace, L., Y. Ottaviano, and C. Kondor-Koch. 1982. Identification of a major polypeptide of the nuclear pore complex. *J. Cell Biol.* 95:826–837.
10. Hertig, A. T. 1968. The primary human oocyte: some observations on the fine structure of Balbiani's vitelline body and the origin of the annulate lamellae. *Am. J. Anat.* 122:107–138.
11. Illmensee, K., A. P. Mahowald, and M. R. Loomis. 1976. The ontogeny of germ plasm during oogenesis in *Drosophila. Dev. Biol.* 49:40–65.
12. Kessel, R. G. 1963. Electron microscope studies on the origin of annulate lamellae in oocytes of *Necturus. J. Cell Biol.* 19:391–414.
13. Kessel, R. G. 1968. Annulate lamellae. *J. Ultrastruct. Res.* Suppl. 10, 1–82.
14. Kessel, R. G. 1981. Origin, differentiation, distribution and possible functional role of annulate lamellae during spermatogenesis in *Drosophila melanogaster. J. Ultrastruct. Res.* 75:72–96.
15. Kessel, R. G. 1983. The structure and function of annulate lamellae: porous cytoplasmic and intranuclear membranes. *Int. Rev. Cytol.* 82:181–303.
16. Kessel, R. G., and H. W. Beams. 1969. Annulate lamellae and "yolk nuclei" in oocytes of the dragonfly, *Libellula pulchella. J. Cell Biol.* 42:185–201.
17. Krohne, G., W. W. Franke, and U. Scheer. 1978. The major polypeptides of the nuclear pore complex. *Exp. Cell Res.* 116:85–102.
18. Mahowald, A. P. 1963. Electron microscopy of the formation of the cellular blastoderm in *Drosophila melanogaster. Exp. Cell Res.* 32:457–468.
19. Mahowald, A. P. 1963. Ultrastructural differentiations during formation of the blastoderm in the *Drosophila melanogaster* embryo. *Dev. Biol.* 8:186–204.
20. Markham, R., S. Frey, and G. Hills. 1963. Methods for the enhancement of image detail and accentuation of structure in electron microscopy. *Virology.* 20:88–102.
21. Maul, G. G. 1970. On the relationship between the Golgi apparatus and annulate lamellae. *J. Ultrastruct. Res.* 30:368–384.
22. Maul, G. G. 1977. The nuclear and cytoplasmic pore complex: structure, dynamics, distribution, and evolution. *Int. Rev. Cytol.* Suppl. 6, 75–186.
23. Okada, E., and C. H. Waddington. 1959. The submicroscopic structure of the *Drosophila* egg. *J. Embryol. Exp. Morphol.* 7:583–597.
24. Rabinowitz, M. 1941. Studies on the cytology and early embryology of the egg of *Drosophila melanogaster. J. Morphol.* 69:1–49.
25. Rickoll, W. L. 1976. Cytoplasmic continuity between embryonic cells and the primative yolk sac during early gastrulation in *Drosophila melanogaster. Dev. Biol.* 49:304–310.
26. Sabatini, D. D., G. Kreibich, T. Morimoto, and M. Adesnik. 1982. Mechanisms for the incorporation of protein in membranes and organelles. *J. Cell Biol.* 92:1–22.
27. Scheer, U. 1972. The ultrastructure of the nuclear envelope of amphibian oocytes. IV. On the chemical nature of the pore complex material. *Z. Zellforsch. Mikrosk. Anat.* 127:127–148.
28. Sonnenblick, B. P. 1950. The early embryology of *Drosophila melanogaster. In* Biology of Drosophila. M. Demerec, editor. John Wiley & Sons, New York. pp. 62–167.
29. Spindler, M., and C. Hemleben. 1982. Formation and possible function of annulate lamellae in a planktic foraminifer. *J. Ultrastruct. Res.* 81:341–350.
30. Stafstrom, J. P., and L. A. Staehelin. 1982. Nuclear division in the syncytial blastoderm embryo of *Drosophila. J. Cell Biol.* 95:304*a*. (Abstr.).
31. Stafstrom, J. P., and L. A. Staehelin. 1984. Dynamics of the nuclear envelope and of nuclear pore complexes during mitosis in the *Drosophila* embryo. *Eur. J. Cell Biol.* In press.
32. Stick, R., and G. Krohne. 1982. Immunological localization of the major architectural protein associated with the nuclear envelope of the *Xenopus laevis* oocyte. *Exp. Cell Res.* 138:319–330.
33. Turner, F. R., and A. P. Mahowald. 1976. Scanning electron microscopy of *Drosophila* embryogenesis. I. The structure of the egg envelopes and the formation of the cellular blastoderm. *Dev. Biol.* 50:95–108.
34. Underwood, E. E. 1970. Quantitative Sterology. Addison-Wesley Co., Reading, MA. 274 pp.
35. Unwin, P. N. T., and R. A. Milligan. 1982. A large particle associated with the perimeter of the nuclear pore complex. *J. Cell Biol.* 93:63–75.
36. Warn, R. M. and R. Magrath. 1982. Observations by a novel method of surface changes during the syncytial blastoderm stage of the *Drosophila* embryo. *Dev. Biol.* 89:540–548.
37. Wischnitzer, S. 1970. The annulate lamellae. *Int. Rev. Cytol.* 27:65–100.
38. Zalokar, M., and I. Erk. 1976. Division and migration of nuclei during early embryogenesis of *Drosophila melanogaster. J. Microsc. Biol. Cell* 25:97–106.
39. Zalokar, M., and I. Erk. 1977. Phase-partition fixation and staining of *Drosophila* eggs. *Stain Technol.* 52:89–95.